Increasing Neurofilament Subunit NF-M Expression Reduces Axonal NF-H, Inhibits Radial Growth, and Results in Neurofilamentous Accumulation in Motor Neurons

Philip C. Wong,*‡ Joe Marszalek,‡§§ Thomas O. Crawford,§ Zuoshang Xu,‡¶ Sung-Tsang Hsieh,§‖ John W. Griffin,§‖ and Don W. Cleveland‡‖‡‡§§**

Departments of *Pathology, ‡Biological Chemistry, §Neurology, and ‖Neuroscience, Johns Hopkins University School of Medicine, Baltimore, Maryland 21205; ¶Worcester Foundation for Experimental Biology, Shrewsbury, Massachussetts 01545; and **The Ludwig Institute for Cancer Research, ‡‡Departments of Medicine and Neuroscience, and §§Division of Cellular and Molecular Medicine, University of California at San Diego, La Jolla, California 92093

Abstract. The carboxy-terminal tail domains of neurofilament subunits neurofilament NF-M and NF-H have been postulated to be responsible for the modulation of axonal caliber. To test how subunit composition affects caliber, transgenic mice were generated to increase axonal NF-M. Total neurofilament subunit content in motor and sensory axons remained essentially unchanged, but increases in NF-M were offset by proportionate decreases in both NF-H and axonal cross-sectional area. Increase in NF-M did not affect the level of phosphorylation of NF-H. This indicates that (*a*) in vivo NF-H and NF-M compete either for coassembly with a limiting amount of NF-L or as substrates for axonal transport, and (*b*) NF-H abundance is a primary determinant of axonal caliber. Despite inhibition of radial growth, increase in NF-M and reduction in axonal NF-H did not affect nearest neighbor spacing between neurofilaments, indicating that cross-bridging between nearest neighbors does not play a crucial role in radial growth. Increase in NF-M did not result in an overt phenotype or neuronal loss, although filamentous swellings in perikarya and proximal axons of motor neurons were frequently found.

NEUROFILAMENTS, the 8–10-nm intermediate filaments of most neurons, are coassembled from three subunits, NF-L, NF-M, and NF-H, with apparent molecular masses of 68, 150, and 200 kD, respectively. While all three proteins have the ~310–amino acid conserved helical domain that is shared by most cytoplasmic intermediate filament subunits, they differ in size mainly by their carboxy-terminal tail domains (Geisler et al., 1983). In mature myelinated axons, neurofilaments are assembled into parallel arrays of long polymers, and are the most abundant cytoskeletal elements, outnumbering microtubules by up to an order of magnitude. The caliber of its axon is an important feature of a neuron because axonal diameter directly governs conduction velocity in myelinated fibers (Gasser and Grundfest, 1939), and may be a trigger for myelination (Arbuthnott et al., 1980; Voyvodic, 1989). An initial proposal that neurofilaments are a major determinant of axon caliber arose from observing a nearly constant density of neurofilaments during the axonal radial growth that begins during myelination and continues throughout adult life (Friede and Samorajski, 1970; Hoffman et al., 1987; Cleveland et al., 1991). It is now apparent that neurofilament content is a primary influence, and not a consequence, of axonal caliber. This has been proven unequivocally to be true in a mutant Japanese quail, in which premature translation termination of NF-L blocks filament assembly (Ohara et al., 1993), and the resultant axons fail to grow radially (Sakaguchi et al., 1993). This has also been shown in mice, where the expression of a mutant NF-H subunit fused to the full coding sequence of β-galactosidase blocks filament transport into axons and profoundly inhibits radial growth (Eyer and Peterson, 1994).

It is also now clear that the general relationship of neurofilament content and caliber is modulated by the relative degree of phosphorylation of NF-M and NF-H. In vitro assembly studies have shown that the extended carboxy-terminal tail domains of NF-M and NF-H are responsible for the formation of side arm structures that protrude from the core 10-nm filament (Geisler et al., 1984; Hirokawa et al., 1984). These side arms may modulate axonal caliber by regulating the spacing between adjacent neurofilaments and/or spacing between neurofilaments and other axonal components. Since the tail domain of NF-H (and to a lesser extent, NF-M) contains multiple repeats of lysine-serine-

Address all correspondence to Dr. Don Cleveland, Ludwig Institute/UCSD, 3080 CMM-East, Mailcode 0660, 9500 Gilman Drive, La Jolla, CA 92093. Tel.: (619) 534-7802. Fax: (619) 534-7659.

proline (Julien et al., 1988; Lees et al., 1988), which provide potential phosphorylation sites (Geisler et al., 1983; Lees et al., 1988), phosphorylation is an attractive candidate for regulating filament interactions. Evidence supporting the idea that phosphorylation can regulate axonal caliber has emerged from the Trembler mouse. Hypomyelination in this mutant mouse correlates with reduction in phosphorylation of neurofilaments and inhibition of radial growth (de Waegh et al., 1992). Further, unmyelinated initial axonal segments have unphosphorylated neurofilaments that are closely packed, and are smaller in diameter than the adjacent myelinated segments (Hsieh et al., 1994; Nixon et al., 1994).

An important remaining question is how neurofilament investment defines caliber, and what role individual subunits play in the event. There have been no previous investigations in which selective reduction in NF-H content was achieved. Similarly, there are no previous assessments of the effect of modifying the content of individual neurofilament subunits on axonal caliber. To begin to evaluate these questions, we have now used an epitope-tagged NF-M subunit to increase NF-M levels in transgenic mice and to analyze the effect of altered neurofilament subunit content on radial growth of motor and sensory axons and on filament–filament spacing.

Materials and Methods

Construction of Transgenic Mice Expression pMSV-NFM-CΔ50

Plasmid pMSV-NFM-CΔ50 encoding a murine NF-M in which the carboxy-terminal 50 amino acids were substituted with a 12–amino acid *myc*-epitope tag has been previously described (Wong and Cleveland, 1990). This hybrid NF-M gene, which also contains a murine sarcoma virus (MSV)[1] promoter substituted in place of the proximal NF-M promoter domain, was excised using ClaI and BamHI, gel purified, and microinjected into one–cell stage, hybrid (C57 B6/A) mouse embryos as previously described (Monteiro et al., 1990). Founder mice were unambiguously identified to be transgenic by genomic DNA blotting of DNA isolated from mouse tail (Xu et al., 1993).

SDS-PAGE and Immunoblotting

Total protein extracts from mouse tissues were homogenized in buffer containing 25 mM sodium phosphate pH 7.2, 5 mM EGTA, 1% SDS and 1 mM PMSF and boiled for 10 min. After determining the protein concentration using the bicinchronic–acid assay (Smith et al., 1985), 20 μg of total protein for each tissue was loaded onto a 7.5% polyacrylamide gel, electrophoresed, and transferred onto nitrocellulose filters as previously described (Lopata and Cleveland, 1987). Endogenous NF-M and NFM-CΔ50 were detected using a mAb against NF-M (Boehringer Mannheim Corp., Biochemicals Division, Indianapolis, IN) and NFM-CΔ50 was detected specifically using mAb 9E10 (Evan et al., 1985) followed by ^{125}I-labeled sheep anti–mouse. Quantitative immunoblotting was performed using a dilution series of known amounts of NF-L, NF-M, NF-H, and *myc*-trpE fusion protein standards electrophoresed on the same blot. Signals were quantified using a PhosphorImager (Molecular Dynamics, Inc., Sunnyvale, CA).

Immunocytochemistry

Immunocytochemistry on 1-μm cryosections was performed according to procedures reported previously (Stoll et al., 1989). Briefly, sciatic nerves were infiltrated for 1 d each with 1, 2, and 2.3 M sucrose in 30% polyvinylpyrrolidone. The specimens were frozen in liquid nitrogen and 1-μm sections were cut with an ultramicrotome (Reichert Scientific Instruments, Div. Warner-Lambert Technologies, Inc., Buffalo, NY) maintained at −90°C. The sections were transferred in sucrose-containing loops to gelatin-subbed slides and stained by the avidin–biotin–peroxidase complex technique (Hsu et al., 1981).

Immunofluorescence and Confocal Laser Scanning Microscopy

Dissected spinal cords were cryoprotected for 24 h in PBS containing 20% glycerol and then sectioned with a freezing microtome. 40-μm-thick sections were rinsed in PBS, incubated for 24 h in PBS containing 2.5% Triton X-100, and then blocked for 30 min with 5% normal horse serum. Sections were incubated for 24 h at 4°C in 1% Triton X-100/PBS plus a combination of a mAb against an epitope tag from human *myc* (9E10; Evan et al., 1985) and a rabbit polyclonal antibody generated against a 15-mer oligopeptide (CYEKTTEDKATKGEK) whose final 13 amino acids correspond to the extreme carboxy terminus of murine NF-H (see Xu et al., 1993). Sections were washed for 2 h in a mixture of FITC–sheep anti–mouse and Texas red–donkey anti–rabbit secondary antibodies (Amersham Corp., Arlington Heights, IL). Finally, the sections were washed in PBS and mounted in a fade-resisting mounting medium containing paraphenylene diamine.

Sections were examined either with standard epifluorescence on a microscope (BH2; Olympus Corporation of America, New Hyde Park, NY) or with a confocal laser scanning microscope (Leica Inc., Deerfield, NY). For the latter, optical sections of ~1 μm thick were collected using a line averaging technique. The Texas red and FITC images were collected simultaneously.

Electron Microscopy, Morphological and Morphometric Analysis

For electron microscopy, tissues were fixed by intracardial perfusion with 0.1 M sodium phosphate (pH 7.6), 4% paraformaldehyde, and 2.5% glutaraldehyde. Tissue samples removed after dissection were immersed in the same fixative for 24 h at 4°C, postfixed for 2 h with 2% osmium tetroxide in 0.1 M phosphate buffer, dehydrated in a graded alcohol series, and embedded in LX-112 (Ladd Research Industries, Inc., Burlington, VT). 1-μm sections were stained with toluidine blue and examined by light microscopy; subsequent thin sections (100 nm) were cut and stained with uranyl acetate and lead citrate, and examined in an electron microscope (H-600; Hitachi Instruments, Inc., San Jose, CA).

Microscopic video images of the 1-μm sections at a light magnification of 100 were digitized using a frame grabber board and image analysis software (Bioquant; R&M Biometrics, Inc., Memphis, TN). The cross-sectional axonal area of myelinated axons >1.5 μm^2 were measured in continuous nonoverlapping fields with center-of-gravity exclusion to avoid double counting. The illumination and optimum gray-scale pixel value for discrimination of the myelin/axon border was chosen independently for each field to minimize systematic bias for a section. Results are reported as the diameter of a circle of equivalent area to the axon.

Analysis of Filament Spacing: Nearest Neighbor Analysis

To measure nearest neighbor distances between neurofilaments, cross sections of axons >3.0 μm in diameter were photographed at a magnification of 20,000 and enlarged an additional fivefold by printing. Neurofilaments were identified in these end-on views as dots of ~10 nm in diameter. Positions of neurofilaments were marked by puncturing the print with a pushpin. By laying the final prints on a light box, neurofilament positions could easily be imaged using a CCD camera, digitized using image analysis software (Bioquant), and nearest neighbor distances calculated for each filament.

Results

Expression of an Epitope-tagged, Assembly Competent NF-M in Neurons of Transgenic Mice

To examine the consequence of expressing an epitope-tagged NF-M subunit in a true in vivo context, transgenic mice were produced that carry an NF-M transgene in which

1. *Abbreviations used in this paper*: ALS, amyotrophic lateral sclerosis; MSV, murine sarcoma virus.

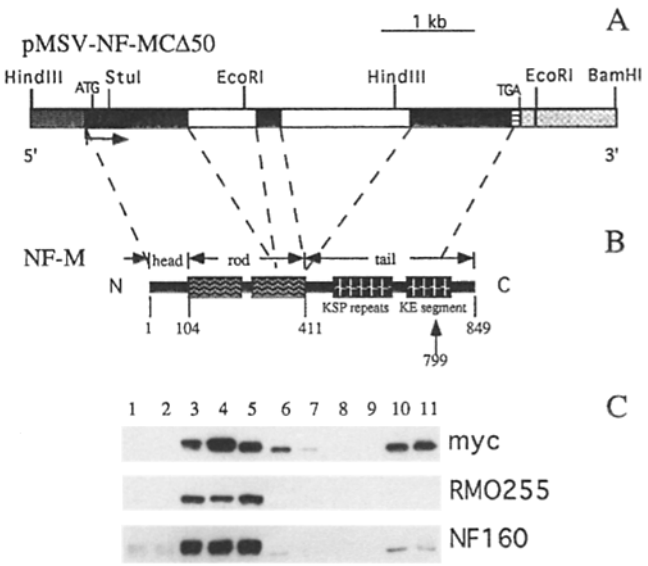

Figure 1. The MSV-NFM-CΔ50 gene, the NF-M polypeptide, and accumulation of epitope-tagged NFM in transgenic mice. (*A*) Schematic drawing of the pMSV-NFM-CΔ50 gene in which the sequences encoding the carboxy-terminal 50 amino acids of NF-M as well as the entire 3′ untranslated and 3′ gene flanking regions have been replaced by sequences encoding a 12–amino acid epitope tag (MEQKLISEEDLN) followed by a TGA stop codon, and the 3′untranslated and 3′ flanking regions of the mouse NF-L gene. *Darkly stippled domain*, MSV promoter; *filled domains*, NF-M exons; *open domains*, NF-M introns; *horizontally striped domain*, myc epitope tag; *stippled domain*, NF-L 3′ untranslated and flanking region. (*B*) Schematic drawing of the NF-M polypeptide. The helical rod domain is bounded by amino acids 104–411. The tail domain is characterized by a phosphorylated domain containing lysine-serine-proline repeats (amino acids 500–610) and a region containing a highly conserved domain rich in lysine and glutamic acid (amino acids 758–838). The deletion end point (and site of epitope tag addition) for the NFM-CΔ50 polypeptide is indicated by the arrow. (*C*) 20 μg of total proteins extracted from various tissues of a 1.5-mo-old NFM-CΔ50(42) mouse were separated on a 6% polyacrylamide gel and immunoblotted using (*top row*) the myc-9E10 antibody recognizing only the NFM-CΔ50 transgenic product, (*middle row*) the RMO255 mAb (kindly provided by V. M.-Y. Lee) which binds only to the endogenous NF-M, or (*bottom row*) an anti-NF160 mAb (Boehringer Mannheim Corp.) which recognizes both the transgenic product and the endogenous NF-M. Lane *1*: cerebral cortex; lane *2*: cerebellum; lane *3*: optic nerve; lane *4*: sciatic nerve; lane *5*: spinal cord; lane *6*: skeletal muscle; lane *7*: kidney; lane *8*: spleen; lane *9*: liver; lane *10*: heart; lane *11*: eye.

the NF-M promoter was substituted with the promoter from MSV. This hybrid gene, MSV-NFM-CΔ50 (Fig. 1 *A*), encodes a mouse NF-M subunit (Fig. 1 *B*) that is identical to the endogenous mouse NF-M, except for substitution of the carboxy-terminal 50 amino acids of the 438–amino acid tail domain with a 12–amino acid epitope tag (from human myc; see Materials and Methods). The resultant NF-M polypeptide contains intact head and rod domains required for filament assembly and transfection analyses into cells expressing vimentin (Wong and Cleveland, 1990), NF-L (Lee et al., 1993), or NF-L and NF-H (data not shown) have demonstrated it to coassemble perfectly into extended arrays of cytoplasmic filaments. Further, use of baculovirus to coexpress NF-L and a myc-tagged NF-M truncated by 95 amino acids yields crossbridged filaments whose ultrastructure and spacing precisely reproduce that seen for NF-L and wild-type NF-M (Nakagawa et al., 1995). In view of this, it seems likely that the epitope-tagged subunit shares most or all of the assembly and functional properties of the wild-type subunit.

12 lines of mice were established using methods previously described (Monteiro et al., 1990) and the two highest expressing lines NFM-CΔ50(2) and NFM-CΔ50(42) were examined in detail. To determine in what tissues and to what level the transgene-encoded NF-M was expressed, whole-cell proteins from 11 different tissues from both transgenic lines 2 and 42 were immunoblotted with antibodies recognizing the epitope tag on transgenic NF-M. Fig. 1 *C* displays the results for an 1.5-mo-old animal from line 42. Similar to the neuron-specific expression of the endogenous NF-M subunits (identified by antibody RMO255; Balin and Lee, 1991), an antibody to the myc epitope tag revealed transgenic NF-M to be found primarily in nervous tissues (e.g., optic nerve, sciatic nerve, spinal cord; Fig. 1 *C*, lanes *3–5*). Using known amounts of purified NF-M or recombinant, epitope-tagged protein as quantification standards and an antibody (RMO255; Balin and Lee, 1991) that binds at the carboxy terminus of NF-M truncated from the transgene-encoded NF-M, phosphorimaging was used to determine that transgenic NF-M accumulated to ~180% the level of endogenous NF-M in sciatic nerve. As seen previously with other MSV-promoted genes (e.g., Monteiro et al., 1990), transgene expression was also observed in some nonneuronal tissues (between ≈0.05 and 0.5% of total cell protein in skeletal muscle, kidney, cardiac muscle, and eye) (Fig. 1 *C*, top row, lanes *6*, *7*, *10*, *11*). In skeletal muscle, transgene expression progressively declined with age, becoming undetectable by three months (not shown).

To determine in neuronal tissues whether the transgene product was expressed solely or predominantly in the neurons, sciatic nerves and spinal cords from control and NFM-CΔ50 mice were cryoprotected, and frozen sections were immunostained for the transgene product or for endogenous NF-H. In sciatic nerve (Fig. 2 *B*), both large and small caliber axons, but not Schwann cells, stained heavily with an mAb (9E10) that recognizes the transgene epitope tag. No such signal was detected in any axon from control nerve (Fig. 2 *A*), although using a mAb specific for phosphorylated NF-H (SMI-31; Sternberger and Sternberger, 1983), all axons from both control and transgenic nerves stained intensely (Fig. 2, *C* and *D*). These results reveal that transgenic NFM-CΔ50 apparently accumulates to comparable levels in most of the axons comprising the nerve.

Sections of spinal cord also yielded intense staining in axons (Fig. 2 *F*, *inset*) throughout the cords of transgenic animals, as well as in motor neuron perikarya (arrows, Fig. 2 *F*). Furthermore, with the epitope tag antibody and a polyclonal antibody generated against the carboxy-terminal 15 amino acids of NF-H (Xu et al., 1993), confocal microscopy of these same samples revealed that NFM-CΔ50 (Fig. 2 *G*) colocalized with endogenous NF-H (Fig. 2 *H*). Similar results were obtained when NFM-CΔ50 localization was compared with NF-L (not shown). Taken to-

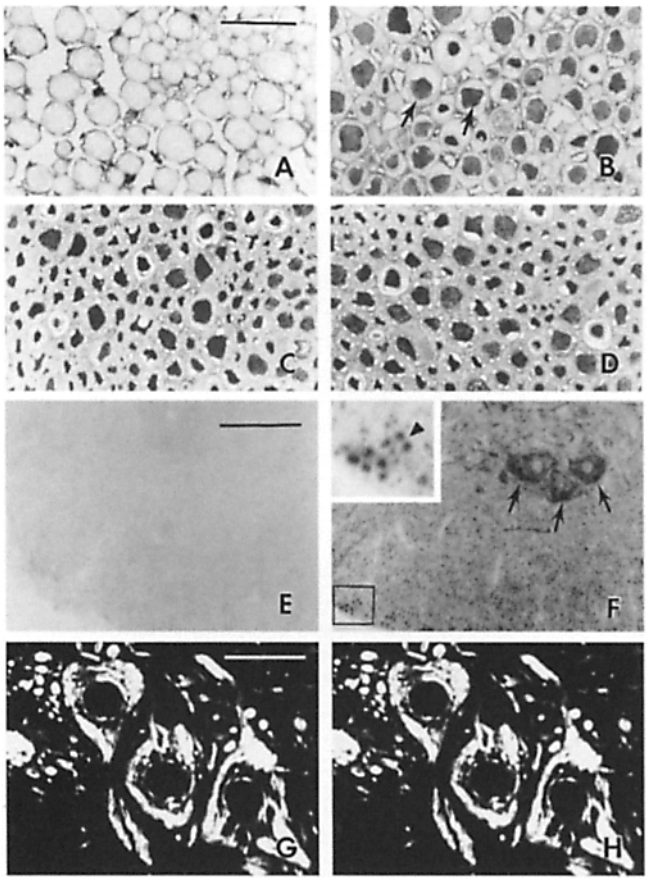

Figure 2. Transgenic NFM-CΔ50 accumulates in motor neuron cell bodies and axons of the spinal cord and sciatic nerve. (*A–D*) Frozen sections (1 μm) of sciatic nerves from 2-mo-old control (*A* and *C*) and NFM-CΔ50(42) (*B* and *D*) mice stained (*A* and *B*) with an mAb (9E10) that recognizes the epitope tag on NFM-CΔ50 and (*C* and *D*) an anti-NF-H (SMI-31) mAb. Arrows in (*B*) point to two of the many intensely stained axons in the NFM-CΔ50(42) mouse. Bar, 20 μm. (*E* and *F*) Frozen sections (40 μm) of spinal cords from (*E*) control and (*F*) NFM-CΔ50(2) mice (1.5-mo-old) stained with the mAb recognizing the NFM-CΔ50 epitope tag. Arrows point to a cluster of three motor neuron cell bodies with abundant NFM-CΔ50, and the arrowhead in the inset highlight the axons with accumulation of the transgene product. Bar, 100 μm. (*G* and *H*) Anterior horn motor neurons from NFM-CΔ50(2) spinal cord (as in *F*) subjected to indirect double immunofluorescence and confocal microscopy. The section was costained for both the transgenic product using (*G*) the epitope tag antibody 9E10 and (*H*) a polyclonal antibody produced against carboxy terminus of mouse NF-H, followed by (*G*) fluorescein-conjugated horse anti–mouse IgG and (*H*) Texas red–conjugated goat anti–rabbit IgG. Bar, 50 μm.

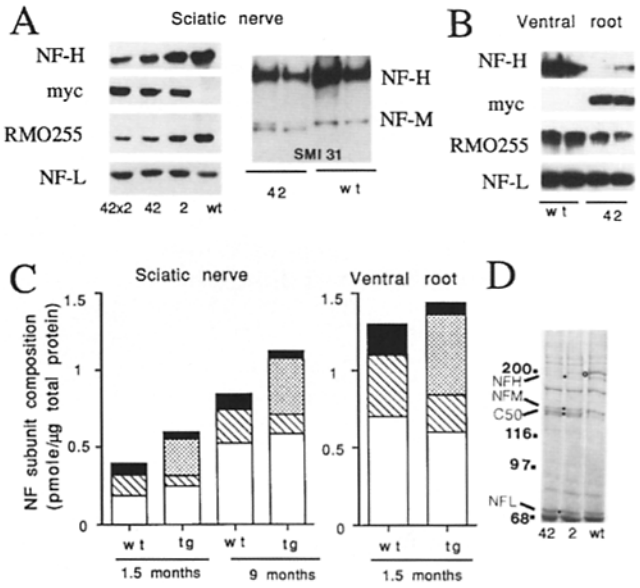

Figure 3. Expression of NFM-CΔ50 decreases axonal NF-H accumulation in sciatic nerves and ventral roots. (*A*) (*left*) 10 μg of total protein extracts of sciatic nerve from 1.5-mo-old mice carrying both line 2 and line 42 transgenes (*42 × 2*), the line 42 transgene only (*42*), the line 2 transgene only (*2*), or age-matched wild-type (*wt*) mice were immunoblotted with either (*left*) a mAb against NF-L, the myc-9E10 mAb, the RMO255 mAb, followed by rabbit anti–mouse secondary antibody and ^{125}I-labeled protein A, or a polyclonal, phosphorylation-independent antibody against NF-H followed by ^{125}I-labeled protein A. A series of twofold dilutions of a bacterial extract containing a fusion protein carrying the epitope tag or purified wild-type mouse neurofilaments were immunoblotted in parallel for quantification. (*Right*) Similar blots probed with the phosphorylation-dependent neurofilament antibody SMI-31. (*B*) Protein blots similar to *A* except from extracts of ventral roots. Samples shown represent independent analyses from two wild-type and two transgenic animals. (*C*) Quantitative analysis (via phosphorimaging) of blots similar to those in (*A* and *B*) are displayed for wild-type (*wt*) and transgenic (*tg*) NFM-CΔ50(42) mice at 1.5 or 9 months-of-age. The neurofilament subunit composition in moles are normalized to total protein. Each point represents the average of immunoblot quantifications of nerve extracts from three different mice for each group. Standard errors for these measurements are given in Table I. *Open domains*, NF-L; *striped domains*, NF-M; *stippled domains*, NFM-CΔ50, and *solid domains*, NF-H. (*D*) Coomassie blue staining of sciatic nerve extracts from lines 42, 2, and wild-type mice. *NFH*: endogenous NF-H; *NF-M*: endogenous NFM; *C50*: transgenic NFM-CΔ50; and *NFL*: endogenous NF-L. Closed circles indicate the bands corresponding to the neurofilament subunits. Open circle denotes a nonneurofilament protein migrating close to NF-H and whose abundance is highly variable in animals of the same genotype. Molecular mass standards are denoted at the left (kD).

gether, these immunocytochemical analyses demonstrate that the transgenic product NFM-CΔ50 is expressed primarily in neurons, is transported into axons, and is colocalized (presumably coassembled) with endogenous neurofilament subunits both in cell bodies and in axons.

Expression of NFM-CΔ50 Reduces Axonal Accumulation of Wild-type NF-H and Inhibits Radial Growth

For both transgenic lines, parallel blots (Fig. 3, *A–C*) were performed to quantify the accumulation of endogenous NF-L, NF-M, and NF-H, as well as transgene-encoded NF-M in sciatic nerve and in L5 ventral root. Measurement of abundance of each neurofilament subunit in each animal was performed in duplicate and quantified by phosphorimaging using standards derived from serial dilutions of known amounts of purified wild-type neurofilament subunits or a bacterially produced fusion protein carrying the epitope

tag. For the ventral root, this revealed (Fig. 3, *B* and right-hand portion of *C*) that in line 42 at 1.5 mo of age, neuronal expression of transgenic NF-M amounted to ~130% the level of NF-M in nontransgenic littermates. Partially compensating for the transgene accumulation, endogenous NF-M levels in the transgenic animals declined to ~60% of the normal level, resulting in a total NF-M subunit level of ~190% of the wild-type level in the transgenic ventral root. Using a phosphorylation-independent antibody to the carboxy-terminal 15 amino acids of NF-H (which lie 207 amino acids from the lysine–serine–proline phosphorylation domain), axonal NF-H level was found to be markedly reduced (Fig. 3, *B* and *C*), falling to only ~40% of that in the nontransgenic control. NF-L levels were not changed significantly in the transgenic ventral root (to ~90% of wild-type).

Similar examination of sciatic nerves from two independent measurements from six transgenic animals (line 42) up to nine months of age (Fig. 3, *A* and *C*) revealed that while transgenic NF-M levels continued to increase during aging (from 180% at 1.5 mo to ~230% of NF-M in wild-type mice), axonal levels of endogenous NF-M and NF-H subunits remained low (~50% of that in control animals). NF-L levels were elevated slightly (~25% at 1.5 months). Coomassie staining of sciatic nerve extracts (Fig. 3 *D*) confirmed that accumulation of transgenic NF-M was accompanied by approximate twofold decreases in both endogenous NF-H and NF-M, while NF-L levels were unaltered. Immunoblotting with an NF-H antibody (SMI-31) that recognizes only phosphorylated NF-H (Fig. 3 *A*, *right*) revealed the same twofold diminution as did the phosphorylation-independent antibodies (Fig. 3 *A*, *top row*, *left*); hence, the average degree of phosphorylation of each NF-H polypeptide was equivalent in wild-type and NF-M transgenic nerves.

Inspection of motor axons in ventral roots and sensory axons in dorsal roots of 1.5-mo-old transgenic animals revealed an obvious difference between wild-type and transgenic NFM-CΔ50 lines 2 or 42. The diameters of the myelinated axons of the transgenic animals were markedly smaller (shown in Fig. 4 for line 42). Detailed morphometric analysis to measure the area of every myelinated axon within a ventral root confirmed this initial impression (Fig. 5, *A* and *B*): although the smallest caliber axons were unchanged in abundance or diameter, the radial growth that accompanies myelination during the first two to three postnatal weeks was reduced significantly in the transgenic axons. At 1.5 mo of age, despite an increased content of NF-M (representing the combination of transgenic and endogenous NF-M; see above, Fig. 3 *C*) and a normal level of NF-L, the average calibers of the largest myelinated axons in the L5 ventral root were only ~3.5 μm in the transgenic animals compared with ~5 μm in littermate controls (Fig. 5 *A*). This corresponds to an axonal cross-sectional area in the transgenic mice of only ~50% that of the wild-type. The substantially reduced radial growth was paralleled by the >50% diminution of axonal NF-H (Fig. 3, *B* and *C*), a finding strongly suggesting that the NF-H subunit is a major determinant for the normal radial growth phase of an axon.

Measurement of the total number of axons between control and transgenic nerve root revealed them to be essentially identical (i.e., 930 ± 36 and 945 ± 36, respectively, for the L5 root; see Table I). Hence, the transgene-dependent shift in axon caliber cannot be due to selective loss of large myelinated fibers. Nor is reduction in caliber likely to be due to the replacement of large fibers with regenerating sprouts, since myelin sheath thicknesses are not altered, and inspection of roots and nerves failed to reveal the presence of degenerating axons (see below). As the animals age, there was a continuing 1.7–2-fold transgene-dependent inhibition of growth in axonal cross-sectional area, with the average diameters of the largest myelinated axons at 9 mo remaining smaller in transgenic animals (~8 μm in the transgenic mice compared with ~10 μm in controls; Fig. 5 *B*). Retardation of radial growth continued to correlate with reduction in the level of axonal NF-H (Fig. 3 *C*), while the overall molar level of neurofilament subunits was similar in NF-M transgenic and control mice.

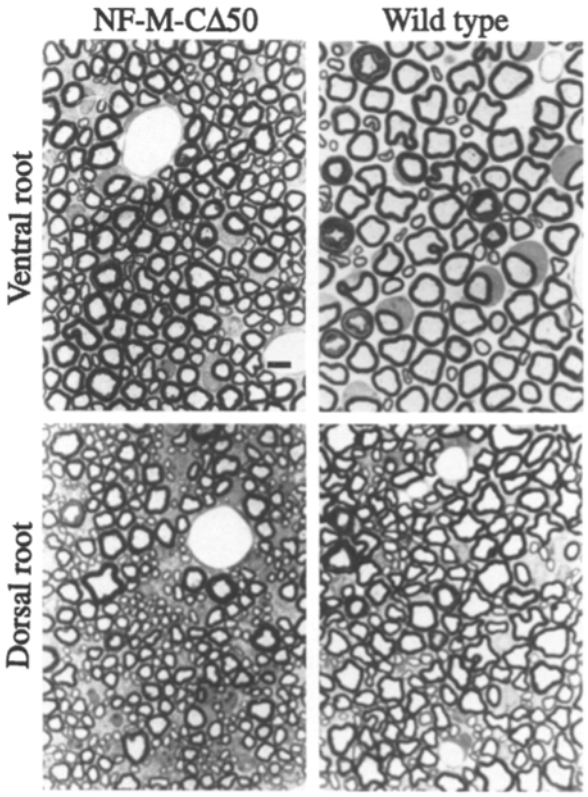

Figure 4. Smaller axonal calibers in motor and sensory axons in mice expressing NFM-CΔ50. Light micrographs display cross sections from dorsal or ventral roots from 1.5-mo-old mice from line NFM-CΔ50(42) or wild-type mice. Bar, 5 μm.

Nearest Neighbor Spacing between Neurofilaments Is Unaffected by Increase in Axonal NF-M and Concomitant Reduction in NF-H

To examine the mechanism through which increase in axonal NF-M and reduction in NF-H inhibit neurofilament-dependent radial growth, the distribution of filaments was examined in cross sections of ventral roots from wild-type and NF-M transgenic animals. This revealed a similar packing of filaments between wild-type (Fig. 6 *A*) and

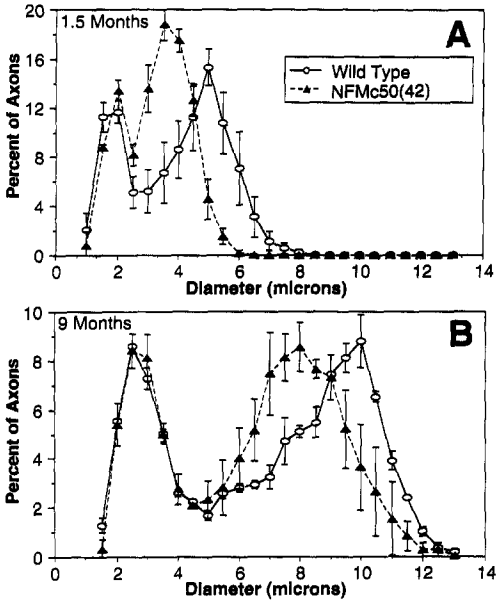

Figure 5. Smaller axonal calibers in motor and sensory axons in mice expressing NFM-CΔ50. Quantitative analysis of axon diameters in L5 ventral roots from control and NFM-CΔ50(42) transgenic animals at 1.5 (*A*) and at 9 months of age (*B*). Each frequency plot of axon diameter represents the average values of three animals, except for the 9-mo-old control group (two animals).

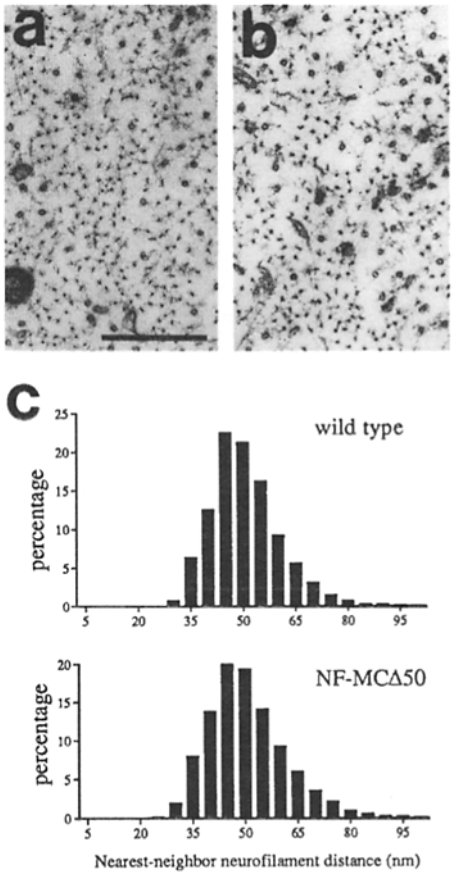

Figure 6. Neurofilament organization in axons from wild-type mice or mice expressing elevated levels of NFM-CΔ50. Axoplasm from cross section of an L5 ventral root axon from a 1.5-mo-old (*a*) wild-type or (*b*) NFM-CΔ50 mouse. Bar, 0.5 μm. (*c*) The distribution of nearest neighbor distances between neurofilaments in ventral root axons from (*top*) wild-type or (*bottom*) NFM-CΔ50(42) mice.

transgenic (Fig. 6 *B*) axons. As one plausible hypothesis was that the heavily phosphorylated tail of NF-H may determine interfilament distance and specify radial growth by forming direct crossbridges between adjacent filaments (e.g., as initially proposed by Hirokawa al., 1984), we examined how diminution of NF-H affects nearest neighbor filament spacing. Positions of all neurofilaments within 10 ventral root axons were established and the distribution of nearest neighbors calculated (Fig. 6 *C*). Despite an ~50% reduction in NF-H (Fig. 3) and a corresponding inhibition of radial growth (Fig. 5), the distributions of nearest interfilament spacings were indistinguishable between NF-M transgenic and littermate control mice (Fig. 6 *C*).

Expression of NFM-CΔ50 Generates Filament Accumulation in Cell Bodies and Proximal Axons

No overt phenotype was observed in NF-M mice at any point between 1.5 and 24 mo of age. However, to assess

Table I. Neurofilament Content, Axonal Caliber and Pathology in NF-M Transgenic Mice

	mouse line			
	NFM–CΔ50 (42)		Wild type	
	1.5 mo	9 mo	1.5 mo	9 mo
Axonal swellings	~5/section	~5/section	None	None
Swollen motor neuron perikarya	~10/section	~10/section	None	None
Number of axons in L5 ventral root*	945 (±41)	1035 (±48)	930 (±36)	993 (±16)
Number of axons in L4, L5, and L6 ventral roots*	ND	2396 (±61) ‡2278 (±72)	ND	2366 (±18)
Average axonal area (μm²)	9.42	50.2	19.6	78.5
Average caliber of large diameter axons in ventral root (μm)	3.50	08	5	10
Total NF content in ventral root (pmol/μg)	1.4 (±0.35)	ND	1.30 (±0.29)	ND
NF-H content in ventral root (pmol/μg)	0.08 (±0.02)	ND	0.20 (±0.03)	ND
NF-M content in ventral root (pmol/μg)	0.76 (±0.18)	ND	0.40 (±0.08)	ND
NF-L content in ventral root (pmol/μg)	0.60 (±0.15)	ND	0.70 (±0.18)	ND

*Average of root(s) from at least two animals (±SD).
‡NFM-CΔ50, line 42 × 2.

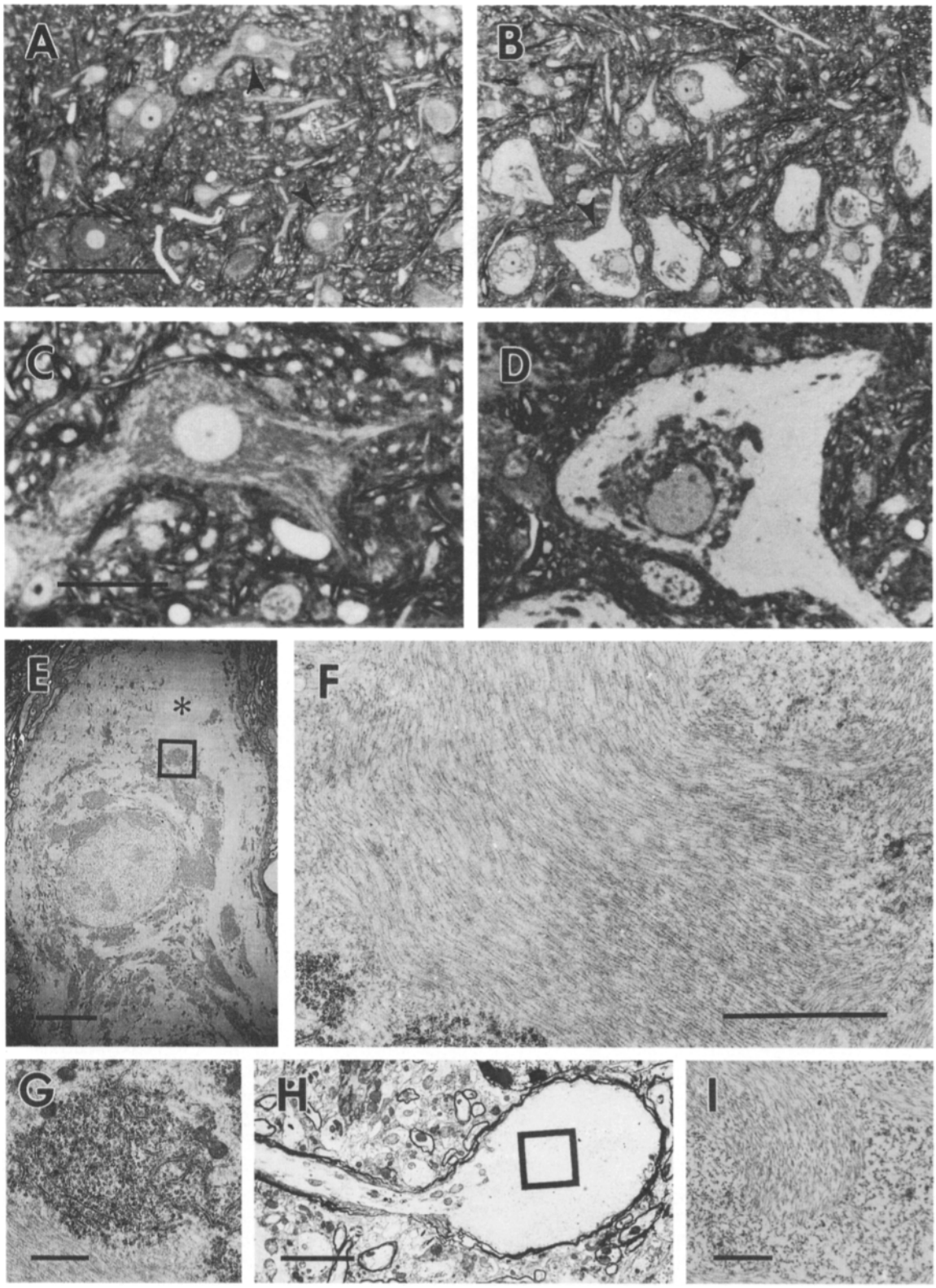

Figure 7. Expression of NFM-CΔ50 generates massive filament accumulation within swollen cell bodies and proximal axons of spinal motor neurons. Toluidine blue–stained (1 μm) sections from the anterior horn of a spinal cord from control (*A* and *C*) and a 1-mo-old MSV-NFM-CΔ50(2) transgenic animal (*B* and *D*). Bar in *A* and *B*, 80 μm; bar in *C* and *D*, 20 μm. (*E–G*) Electron micrographs of a motor neuron from a 1.5-mo-old MSV-NFM-CΔ50(42) transgenic animal. Higher magnification of the boxed areas reveals (*F*) massive accumulation of filaments in the cytoplasm and (*G*) aggregation of RER. Bar in *E*, 10 μm; bar in *F*, 2 μm; bar in *G*, 1 μm. (*H* and *I*) Electron micrographs of a proximal axonal swelling from the same spinal cord as in (*E*). Bar in *H*, 5 μm; bar in *I*, 1 μm.

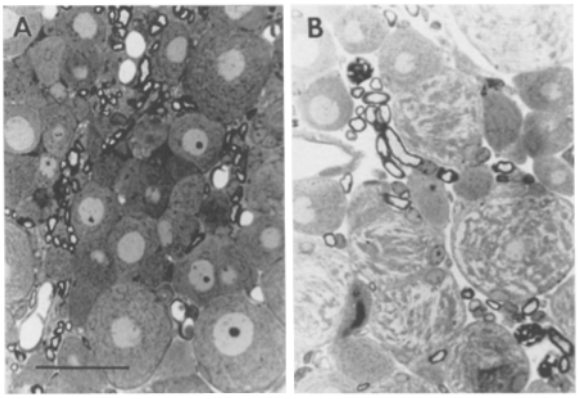

Figure 8. Neurofilamentous accumulation in large sensory neurons of dorsal root ganglia. 1-μm sections of dorsal root ganglia from control (*A*) and 1.5-mo-old MSV-NFM-CΔ50(42) transgenic (*B*) animal stained with toluidine blue. Bar, 30 μm.

whether there were morphological consequences of NFM-CΔ50 expression in neurons, eight transgenic mice from both lines 42 and 2, as well as age-matched controls, were perfused at various ages (postnatal d 26 to 5 mo) and their tissues were processed for both light and electron microscopy (summarized in Table I). Striking morphological alterations in NFM-CΔ50(2) mice were observed as early as day 26 in the anterior horn motor neurons. Most of the motor neurons displayed distended, swollen perikarya (Fig. 7, *B* and *D*) compared with nontransgenic littermates (Fig. 7, *A* and *C*). At the electron microscopic level, these swellings consisted of massive bundles of tightly packed filaments (Fig. 7, *E* and *F*). Indirect double immunofluorescence demonstrated that these filament bundles contain both transgene and endogenous NF subunits (see above; Fig. 2, *G* and *H*). Swirls of filaments occupy most of the cytoplasmic volume, which in turn results in the aggregation of RER around the nucleus (Fig. 7 *E*), as well as patches scattered throughout the cytoplasm (see close-up in Fig. 7 *G*). In contrast, the RER is distributed evenly throughout the cytoplasm in wild-type perikarya (not shown). Another prominent characteristic of motor neurons in NFM-CΔ50 mice was numerous proximal axonal swellings (Fig. 7 *H*). When observed at higher magnification, accumulations of massive bundles of filaments were obvious in these swollen axonal segments (Fig. 7 *I*).

To examine whether expression of NFM-CΔ50 also affected neurons besides spinal motor neurons, the nervous system of a mouse from line 2 was surveyed (Fig. 8). Neurofilament masses were readily apparent in other large neurons, including prominent accumulations in the largest sensory neurons of the dorsal root ganglia. Most of these were distended with arrays of neurofilaments (lightly stained areas in Fig. 8 *B*), although examination of the entirety of the dorsal root did not reveal any axonal degeneration. Neurofilamentous accumulation was also observed in other types of neurons, including pyramidal neurons from the hippocampus, the large neurons in the trigeminal sensory nucleus, and the motor neurons in the facial nucleus of the brainstem (data not shown). A common thread among all these different types of neurons that show morphologic abnormalities as a consequence of NFM-CΔ50 accumulation is that they represent large neurons, each with a high normal neurofilament burden.

Neither the perikaryal or axonal accumulations resulted in an elevated frequency of axonal degeneration, as no degenerating axons were observed in examination of the entirety of L4 through L6 ventral roots from two transgenic animals either at 1.5 or 9 months of age. Count of axon number in L5 ventral roots further revealed no significant difference between transgenic and wild-type animals at any age (Table I).

Discussion

To earlier linkage of neurofilament accumulation as an intrinsic determinant of axonal caliber, our present results provide proof that neurofilament subunit composition plays an important role in establishment and maintenance of axonal caliber: at constant NF-L levels and slightly elevated total neurofilament content, transgene-encoded NF-M raised overall NF-M levels, and yet inhibited radial growth concomitant with reduction in endogenous NF-H. The simplest interpretation is that axonal NF-H is the primary determinant of radial growth, while the more abundant NF-L subunit provides the basic framework for core filament assembly. Such a conclusion is also consonant with earlier efforts demonstrating a correlation between radial growth and phosphorylation of the tail domains of NF-M and NF-H both in the initial axonal segment (Hsieh et al., 1994; Nixon et al., 1994), in nodes (Hsieh et al., 1994), and in response to demyelination (deWaegh et al., 1992). It is also consistent with the finding that proximal axons are increased in size after expression of wild-type human NF-H in transgenic mice (Cote et al., 1993) and the severe inhibition of radial growth after blockage of NF-H (along with NF-L and NF-M) transport into axons after expression of a truncated NF-H fused to the entirety of β-galactosidase (Eyer and Peterson, 1994).

The loss of endogenous NF-H as a consequence of increasing NF-M expression, while NF-L levels remain unchanged, demonstrates an in vivo competition between accumulation of NF-M and NF-H. The nature of the competition could arise from competition either as substrates for the slow axonal transport machinery or for coassembly with NF-L, which at least in the transgenic neurons, is present in limiting amounts. The latter view is fully consistent with the finding that assembly of neurofilament networks after expression in nonneuronal cells requires NF-L and substoichiometric amounts of either NF-M or NF-H (Ching and Liem, 1993; Lee et al., 1993).

Although NF-H (and its phosphorylation) must be an important element for specifying caliber, we would note that the evidence does not yet formally exclude a contribution from NF-M, since the partial replacement of endogenous NF-M with the slightly truncated, epitope-tagged NF-M subunit could reduce (or eliminate) such an activity. However, similar tagging (with even significantly larger carboxy-terminal truncations) has not been found to affect coassembly properties with NF-L, either in transfected mammalian cells (Lee et al., 1993) or in insect cells infected with baculoviruses encoding both NF-L and NF-M (Nakagawa et al., 1995). Moreover, in the latter example, filament–filament spacing properties are identical for wild-

type subunits and for NF-M epitope tagged with *myc* and truncated by 95 amino acids (Nakagawa et al., 1995). At a minimum, even if the transgene-encoded NF-M does function slightly aberrantly, a strong conclusion remaining would be that both NF-H and NF-M are necessary for normal radial growth. Since in the absence of neurofilament investment large myelinated axons achieve only ~1/6 of their normal cross-sectional areas either in quails (Sakaguchi et al., 1993) or in mice (Eyer and Peterson, 1994), this would be particularly appealing given that even with depressed NF-H levels, significant growth does still occur in the NF-M transgenic axons both during myelination and increasing in later life (compare Fig. 5, *A* and *B*).

As to the mechanism through which neurofilaments mediate growth in caliber, a plausible view has been that the highly phosphorylated tail domain of NF-H orders axoplasmic structure through interaction (crossbridging) between adjacent neurofilaments. This idea arose initially from demonstration using immunocytochemistry that in vivo crossbridges between filaments were comprised of NF-H tails (Hirokawa et al., 1984). The current finding that nearest neighbor distributions between wild-type and NF-M-transgenic axons are indistinguishable strongly suggests that NF-M- (but not NF-H-) dependent interactions may serve to specify nearest neighbor spacing, while the phosphorylated NF-H tail may establish caliber through a three-dimensional filament scaffold arising from tail-mediated, longer range crossbridging between filaments that are not nearest neighbors and/or through interactions with other axonal components, such as microtubules, cortical actin arrays, and potentially many other components. Further, it seems likely that phosphorylation of the NF-M tail may determine (or at least influence) the minimal interfilament distance. An ~50-nm spacing is found in myelinated axons where NF-M is fully phosphorylated, whereas only an ~30-nm filament–filament spacing is seen where NF-M is unphosphorylated (i.e., the initial axonal segment [Hsieh et al., 1994] and in insect cells expressing NF-L and NF-M [Nakagawa et al., 1995]).

Abnormal neurofilamentous accumulations in the perikarya and proximal axons of motor neurons, an early hallmark of human motor neuron diseases such as amyotrophic lateral sclerosis (ALS) (Carpenter, 1968; Inoue and Hirano, 1979; Hirano et al., 1984 *a*,*b*; Banker, 1986; Saskai et al., 1988; for review see Hirano, 1991), initially suggested that neurofilaments may play an important role in the pathogenesis of this disorder. Clinically characterized by degeneration and loss of motor neurons followed by progressive, denervation-induced muscle atrophy (Tower, 1939; Mulder, 1984, 1986), the mechanism(s) of pathogenesis is unknown, although mutations in superoxide dismutase are known to cause a small percentage of cases (Rosen et al., 1993). Direct evidence that aberrant accumulation of neurofilaments can play an integral part in motor neuron disease has emerged from the efforts of two groups who independently have shown that two- to fourfold overexpression in transgenic mice of either mouse NF-L (Xu et al., 1993) or human NF-H (Cote et al., 1993; Collard et al., 1995) does result in aberrant neurofilamentous accumulations and some of the pathological features that resemble those found in ALS. Moreover, expression of a point mutant in NF-L at the level expected from a single gene in a diploid cell produces not only this pathology, but also selective motor neuron death (Lee et al., 1994). To this, the present results prove that an approximately twofold elevation of NF-M results in altered ratios of the three neurofilament subunits and abnormal filamentous aggregates in neuronal cell bodies and axons. Hence, when combined with the earlier work (Cote et al., 1993; Xu et al., 1993; Collard et al., 1995), significant increases in any neurofilament subunit can produce pathology characteristic of the early phases of motor neuron disease (for review see Hirano, 1991). In each instance, the most severely affected neurons are the large, neurofilament-rich motor neurons, although morphological abnormalities are also found in peripheral sensory neurons and a few other large neurons of the central nervous system that are naturally abundant in neurofilaments. This mimics the pathology reported by a series of workers for the late stages of ALS, where besides prominent defects in motor neurons, there is also evidence demonstrating an involvement of sensory neurons (Kawamura et al., 1981; Averback and Croker, 1982; Radtke et al., 1986).

With regard to how neurofilaments can provoke neuronal failure, only very high doses of NF-L result in disease (Xu et al., 1993), whereas a severalfold smaller molar increase of human NF-H subunits is equally pathogenic in mice (Cote et al., 1993). Despite neurofilament-induced neuronal failure, in neither instance is there significant neuronal death (for NF-L, see Xu et al., 1993; for NF-H, see Fig. 1 *b* of Collard et al., 1995). Increasing NF-M levels, at least to the levels achieved here, does not lead to an overt phenotype or axonal degeneration, despite perikaryal filamentous swellings and a slight increase in the overall axonal burden of filament subunits. A unifying view for how filaments provoke disease would be that it is primarily axonal accumulations that are pathogenic, most probably by an increasing burden of filaments adversely affecting axonal transport. In this view, increasing NF-L may lead to many more axonal filaments, which when present at sufficient levels retard (potentially block) slow axonal transport. For NF-H, whose abundance is known to correlate inversely with the speed of slow transport (Willard and Simon, 1983), increasing its levels in proximal axons and perikarya strongly retards transport (Collard et al., 1995). On the other hand, increasing NF-M would have a much smaller effect for two reasons: (*1*) a limiting level of NF-L prevents additional axonal filament assembly, and (*2*) competition between NF-H and an increased level of NF-M yields decreased axonal NF-H abundance.

In any event, along with earlier reports on NF-L (Xu et al., 1993) and NF-H (Cote et al., 1993), our present results establish that primary changes in abundance of any of the three neurofilament subunits are sufficient to recapitulate some of the early pathologic features observed in motor neuron diseases such as ALS. These findings combine to suggest that even in disorders (like ALS arising from mutation in superoxide dismutase) where accumulation of neurofilaments are secondary to other types of neuronal insult, axonal neurofilament accumulation may play an essential pathogenic role in neuronal failure.

We thank an anonymous reviewer for pointing out to us the potential role of NF-M as a determinant of nearest neighbor filament spacing. We also

thank Dr. Michael Lee for many helpful comments and criticisms over the course of this work, Ms. Janet Folmer for her expert assistance with the electron microscopy, and Dr. Virginia Lee for providing monoclonal antibodies to NF-M.

This work has been supported by grants from the National Institutes of Health (NIH) to D. W. Cleveland and J. W. Griffin. D. W. Cleveland is the recipient of an NIH Jacob Javits Neuroscience Investigator award. P. C. Wong and Z. Xu were supported, in part, by postdoctoral fellowships from the Muscular Dystrophy Association.

Received for publication 10 May 1995 and in revised form 21 June 1995.

References

Arbuthnott, E. R., I. A. Boyd, and K. U. Kalu. 1980. Ultrastructural dimensions of myelinated peripheral nerve fibres in the cat and their relation to conduction velocity. *J. Physiol.* 308:125–157.

Averback, P., and P. Crocker. 1982. Regular involvement of Clarke's nucleus in sporatic amyotrophic lateral sclerosis. *Arch. Neurol.* 39:155–156.

Balin, B. J., and V. M. Lee. 1991. Neurofilament reassembly in vitro: biochemical, morphological, and immuno-electronmicroscopic studies employing monoclonal antibodies to defined epitopes. *Brain Res.* 556:181–195.

Banker, B. Q. 1986. The pathology of the motor neuron disorders. *In* Myology. A. G. Engel and B. Q. Banker, editors. McGraw-Hill Inc. New York. 2031–2066.

Carpenter, S. 1968. Proximal axonal enlargement in motor neuron disease. *Neurology.* 18:841–851.

Ching, G. Y., and R. K. H. Liem. 1993. Assembly of type IV neuronal intermediate filaments in nonneuronal cells in the absence of preexisting cytoplasmic intermediate filaments. *J. Cell Biol.* 122:1323–1335.

Cleveland, D. W., M. J. Monteiro, P. C. Wong, S. R. Gill, J. D. Gearhart, and P. N. Hoffman. 1991. Involvement of neurofilaments in the radial growth of axons. *J. Cell Sci.* 15:85–95.

Collard, J.-F., F. Cote, and J.-P. Julien. 1995. Defective axonal transport in a transgenic mouse model for amyotrophic lateral sclerosis. *Nature (Lond.).* 375:61–64.

Cote, F., J. F. Collard, and J. P. Julien. 1993. Progressive neuronopathy in transgenic mice expressing the human neurofilament heavy gene: a mouse model of amyotrophic lateral sclerosis. *Cell.* 73:35–46.

de Waegh, S. M., V. M.-Y. Lee, and S. T. Brady. 1992. Local modulation of neurofilament phosphorylation, axonal caliber, and slow axonal transport by myelinating Schwann cells. *Cell.* 68:451–463.

Evan, G. I., G. K. Lewis, G. Ramsay, and J. M. Bishop. 1985. Isolation of monoclonal antibodies specific for human c-*myc* proto-oncogene product. *Mol. Cell. Biol.* 5:3610–3616.

Eyer, J., and A. Peterson. 1994. Neurofilament-deficient axons and perikaryal aggregates in viable transgenic mice expressing a neurofilament-β-galactosidase fusion protein. *Neuron.* 12:389–405.

Friede, R. L., and T. Samorajski. 1970. Axon caliber related to neurofilaments and microtubules in sciatic nerve fibers of rats and mice. *Anat. Rec.* 167:379–388.

Gasser, H. S., and H. Grundfest. 1939. Axon diameters in relation to the spike dimensions and the conduction velocity in mammalian A fibers. *Am. J. Physiol.* 127:393–414.

Geisler, N., S. Kaufmann, S. Fischer, U. Plessmann, and K. Weber. 1983. Neurofilament architecture combines structural principles of intermediate filaments with carboxy-terminal extensions increasing in size between triplet proteins. *EMBO (Eur. Mol. Biol. Organ.) J.* 2:1295–1302.

Geisler, N., S. Fisher, J. Vanderkerchove, U. Plessmann, and K. Weber. 1984. Hybrid character of a large neurofilament protein (NF-M): intermediate filament type sequence followed by a long acidic carboxy-terminal extension. *EMBO (Eur. Mol. Biol. Organ.) J.* 3:2701–2706.

Hirokawa, N., M. A. Glicksman, and M. B. Willard. 1984. Organization of mammalian neurofilament polypeptides within the neuronal cytoskeleton. *J. Cell Biol.* 98:1523–1536.

Hirano, A. 1991. Cytopathology of amyotrophic lateral sclerosis. *Adv. Neurol.* 56:91–102.

Hirano, A., H. Donnenfeld, S. Shoichi, and I. Nakano. 1984*a*. Fine structural observations of neurofilamentous changes in amyotrophic lateral sclerosis. *J. Neuropathol. & Exp. Neurol.* 43:461–470.

Hirano, A., I. Nakano, L. T. Kurland, D. W. Mulder, P. W. Holly, and G. Saccomanno. 1984*b*. Fine structural study of neurofibrillary changes in a family with amyotrophic lateral sclerosis. *J. Neuropathol. & Exp. Neurol.* 43:471–480.

Hoffman, P. N., D. W. Cleveland, J. W. Griffin, P. W. Landes, N. J. Cowan, and D. L. Price. 1987. Neurofilament gene expression: a major determinant of axonal caliber. *Proc. Natl. Acad. Sci. USA.* 84:3272–3476.

Hsieh, S.-T., G. J. Kidd, T. O. Crawford, Z.-S. Xu, B. D. Trapp, D. W. Cleveland, and J. W. Griffin. 1994. Regional modulatoin of neurofilament organization by myelination in normal axons. *J. Neurosci.* 14:6392–6401.

Hsu, S. M., L. Raine, and H. Fanger. 1981. The use of avidin-biotin peroxidase complex (ABC) in immunoperoxidase techniques: A comparison between ABC and the unlabeled antibody (PAP) procedures. *J. Histochem. Cytochem.* 29:577–580.

Inoue, K., and A. Hirano. 1979. Early pathological changes of amyotrophic lateral sclerosis: autopsy findings of a case of 10 months' duration. *Neurol. Med. (Tokyo).* 11:448–455.

Julien, J.-P., F. Cote, L. Beaudet, L. Sidky, D. Flavell, F. Grosveld, and W. E. Mushynski. 1988. Sequence and structure of the mouse gene coding for the largest neurofilament subunit. *Gene (Amst.).* 68:307–314.

Kawamura, Y., P. J. Dyck, M. Shimono, H. Okazaki, J. Tateishi, and H. Doi. 1981. Morphometric comparison of the vulnerability of peripheral motor and sensory neurons in amyotrophic lateral sclerosis. *J. Neuropathol. & Exp. Neurol.* 40:667–675.

Lee, M. K., Z. Xu, P. C. Wong, and D. W. Cleveland. 1993. Neurofilaments are obligate heteropolymers in vivo. *J. Cell Biol.* 122:1337–1350.

Lee, M. K., J. R. Marszalek, and D. W. Cleveland. 1994. Expression of a mutant neurofilament subunit causes massive, selective motor neuron death and ALS-like motor neuron disease. *Neuron.* 13:975–988.

Lees, J. F., P. S. Shneidman, S. F. Skuntz, M. J. Carden, and R. A. Lazzarini. 1988. The structure and organization of the human heavy neurofilament subunit (NF-H) and the gene encoding it. *EMBO (Eur. Mol. Biol. Organ.) J.* 7: 1947–1955.

Lopata, M. A., and D. W. Cleveland. 1987. In vivo microtubules are copolymers of available β-tubulin isotypes: localization of each of the six vertebrate β-tubulin isotypes using polyclonal antibodies elicited by synthetic peptide antigens. *J. Cell Biol.* 105:1707–1720.

Monteiro, M. J., P. N. Hoffman, J. D. Gearhart, and D. W. Cleveland. 1990. Expression of NF-L in both neuronal and nonneuronal cells of transgenic mice: increased neurofilament density in axons without affecting caliber. *J. Cell Biol.* 111:1543–1557.

Mulder, D. W. 1984. Motor neuron disease. *In* Peripheral Neurophathy. P. J. Dyck, P. K. Thomas, E. H. Lambert, and R. Bunge, editors. W. B. Saunders Company. Philadelphia. 1525–1536.

Mulder, D. W. 1986. Motor neuron disease in adults. *In* Myology. A. G. Engel and B. Q. Banker, editors. McGraw-Hill Inc., New York. 2013–2029.

Nakagawa, T., J. Chen, Z. Zhang, Y. Kanai, and N. Hirokawa. 1995. Two distinct functions of the carboxyl-terminal tail domain of NF-M upon neurofilament assembly; cross-bridge formation and longitudinal elongation of filaments. *J. Cell Biol.* 129:411–429.

Nixon, R. A., P. A. Paskevich, R. K. Sihag, and C. Y. Thayer. 1994. Phosphorylation on carboxyl terminus domains of neurofilament proteins in retinal ganglion cell neurons in vivo: influences on regional neurofilament accumulation, interneurofilament spacing, and axon caliber. *J. Cell Biol.* 126:1031–1046.

Ohara, O., Y. Gahara, T. Miyake, H. Teraoka, and T. Kitamura. 1993. Neurofilament deficiency in quail caused by nonsense mutation in neurofilament-L gene. *J. Cell Biol.* 121:387–395.

Radtke, R., A. Erwin, and C. Erwin. 1986. Abnormal sensory evoked potentials in amyotrophic lateral sclerosis. *Neurology.* 36:796-801.

Rosen, D. R., T. Siddique, D. Patterson, D. A. Figlewicz, P. Sapp, A. Hentatl, D. Donaldson, J. Goto, J. P. O'Reagan, H.-X. Deng et al. 1993. Mutations in Cu/Zn superoxide dismutase gene are associated with familial amyotrophic lateral sclerosis. *Nature (Lond.).* 362:59–62.

Sakaguchi, T., M. Okada, T. Kitamura, and K. Kawasaki. 1993. Reduced diameter and conduction velocity of myelinated fibers in the sciatic nerve of a neurofilament-deficient mutant quail. *Neurosci. Lett.* 153:65–68.

Sasaki, S., H. Kamei, K. Yamane, and S. Murayama. 1988. Swelling of neuronal processes in motor neuron disease. *Neurology.* 38:1114–1118.

Smith, P. K., P. I. Krhon, G. T. Hermanson, A. K. Mallia, F. H. Gartner, M. D. Provenzaus, E. K. Fujimoto, N. M. Goeke, B. J. Olson, and D. C. Klenk. 1985. Measurement of protein using bicinchonic acid. *Anal. Biochem.* 150: 76–85.

Sternberger, L. A., and N. H. Sternberger. 1983. Monoclonal antibodies distinguish phosphorylated and nonphosphorylated forms of neurofilaments in situ. *Proc. Natl. Acad. Sci. USA.* 80:6126–6130.

Stoll, G., J. W. Griffin, C. Y. Li, and B. D. Trapp. 1989. Wallerian degeneration in the peripheral nervous system: participation of both Schwann cells and macrophages in myelin degradation. *J. Neurocytol.* 18:671–683.

Tower, S. S. 1939. The reaction of muscle to denervation. *Physiol. Rev.* 19:1–48.

Voyvodic, J. T. 1989. Target size regulates caliber and myelination of sympathetic axons. *Nature (Lond.).* 342:430–432.

Willard, M., and C. Simon. 1983. Modulations of neurofilament axonal transport during development of rabbit retinal ganglion cells. *Cell.* 35:551–559.

Wong, P. C., and D. W. Cleveland. 1990. Characterization of dominant and recessive assembly-defective mutations in mouse neurofilament NF-M. *J. Cell Biol.* 111:1987–2003.

Xu, Z.-S., L. C. Cork, J. W. Griffin, and D. W. Cleveland. 1993. Increased expression of neurofilament subunit NF-L produces morphological alterations that resemble the pathology of human motor neuron disease. *Cell.* 73:23–33.